Vertically Aligned Carbon Nanotubes Grown on Graphene Paper as Electrodes in Lithium-Ion Batteries and Dye-Sensitized Solar Cells

ARTICLE *in* ADVANCED ENERGY MATERIALS · JULY 2011

Impact Factor: 16.15 · DOI: 10.1002/aenm.201100001

10 AUTHORS, INCLUDING:

Shisheng Li
National University of Singapore
16 PUBLICATIONS **508** CITATIONS
SEE PROFILE

Yanhong Luo
Chinese Academy of Sciences
94 PUBLICATIONS **3,050** CITATIONS
SEE PROFILE

Wei Lv
Tsinghua University
72 PUBLICATIONS **2,209** CITATIONS
SEE PROFILE

Hui-Ming Cheng
Shenyang National Laboratory for Material…
488 PUBLICATIONS **33,637** CITATIONS
SEE PROFILE

COMMUNICATION

Vertically Aligned Carbon Nanotubes Grown on Graphene Paper as Electrodes in Lithium-Ion Batteries and Dye-Sensitized Solar Cells

Shisheng Li, Yanhong Luo, Wei Lv, Wanjing Yu, Sida Wu, Pengxiang Hou, Quanhong Yang, Qingbo Meng,* Chang Liu,* and Hui-Ming Cheng*

Vertically aligned carbon nanotubes (VACNTs) possess the advantages of a high degree of order, good controllability, and easy manipulation. Thus, their synthesis, properties, and potential for applications have been intensively investigated.[1–5] VACNTs are usually grown by chemical vapor deposition (CVD) on substrates with pre-deposited catalysts. Due to the rigorous CVD synthesis conditions, substrates employed for VACNT growth should be thermally and chemically stable materials, such as SiO_2/Si, Al_2O_3, or quartz. A problem thus arising is that these substrates are usually insulators, which hampers the direct application of VACNTs in those areas that require desirable integrated electrical and thermal conductivities.[6] For example, a mismatching problem often emerges when assembling devices based on VACNTs due to the rigidity and poor conductivity of the substrates. To solve this problem, some researchers have developed multiform but complicated methods to transfer VACNTs from the insulating substrates to conducting substrates by post-synthesis processing, which facilitates the application of VACNTs in some electronic devices, such as field emitters.[7,8] On the other hand, Tatsuki et al. reported direct growth of VACNTs on Ni-based alloy foils.[9] Although excellent field emission homogeneity was demonstrated, the 30 nm thick alumina buffer layer deposited between the metal substrate and catalyst film weakens the electrical contact and mechanical adhesion between the VACNTs and the metal substrate. The incompatible thermal expansion coefficients of alumina and metal may also lead to detaching of the VACNTs and the alumina buffer layer from the metal substrate.

S. S. Li, W. J. Yu, Dr. P. X. Hou, Prof. C. Liu, Prof. H.-M. Cheng
Shenyang National Laboratory of Materials Science
Institute of Metal Research
Chinese Academy of Sciences
72 Wenhua Road, Shenyang 110016, P.R. China
E-mail: cliu@imr.ac.cn
Dr. Y. H. Luo, Prof. Q. B. Meng
Beijing National Laboratory for Condensed Matter Physics
Institute of Physics
Chinese Academy of Sciences
Beijing 100190, P.R. China
E-mail: qbmeng@iphy.ac.cn
W. Lv, S. D. Wu, Prof. Q. H. Yang
School of Chemical Engineering and Technology
Tianjin University
Tianjin 300072, P.R. China
E-mail: qhyangcn@tju.edu.cn

DOI: 10.1002/aenm.201100001

Graphene is a newly discovered 2D carbon material with excellent conductivity, mechanical properties,[10,11] and more importantly, compatibility with CNTs. Therefore, graphene can be an ideal substrate for VACNT growth. Recently, Lee et al. demonstrated the growth of VACNTs on a ~7 nm thick reduced graphene film supported by silicon wafer. The VACNT/graphene hybrid film infiltrated with a poly(dimethyl siloxane) (PDMS) elastomer displayed good mechanical properties, electrical conductivity, and field emission performance.[12] Nitrogen-doped VACNTs grown on mechanically compliant graphene film for a flexible field emitter were also demonstrated by Lee et al.[13] Jeong et al. reported a flexible room temperature NO_2 gas sensor consisting of a VACNT/reduced graphene hybrid film supported by a polyimide substrate.[14] Paul et al. prepared a 3D pillared graphene nanostructure comprising graphene and aligned carbon nanotubes by a one-step CVD method.[15] Zhang et al. demonstrated desirable visible light photocatalytic performance for a 3D pillared CNT/reduced graphene oxide composite material.[16] Fan et al. prepared a 3D CNT/graphene sandwich with short CNT pillars (~100 nm in length) grown between graphene layers or by ultrasonicating purified, short-cut CNTs in a graphene oxide suspension followed by thermal reduction. The sandwich-structured material displayed excellent performance when used as the electrode of a supercapacitor.[17] Although these hybrid carbon nanostructures show excellent performance, the strength of the thin graphene film is not sufficient without a support. To properly maintain its integrity and flexibility, the hybrid film usually needs to be transferred to a flexible substrate[14] or infiltrated with polymer before testing and application.[12]

In this study, we grew VACNTs directly onto a freestanding graphene paper (GP) by using CVD. The GP, consisting of numerous densely packed graphene sheets, is ~3 μm in thickness, which guarantees its easy manipulation as a substrate for CNT growth and further applications. Since the GP is conducting, flexible, and chemically stable, and the VACNTs combine well with the GP, this freestanding hybrid carbon material may show considerable appeal in applications for energy conversion and storage devices. The performance of the VACNT/GP film as an anode in lithium-ion batteries (LIBs) and as a counter electrode in dye-sensitized solar cells (DSSCs) was investigated.

We prepared graphene oxide paper (GOP) through a self-assembly process at the liquid/air interface of an aqueous graphene oxide solution.[18] **Figure 1**a shows the optical image of a GOP strip, which is reddish-brown in color, sub-transparent,

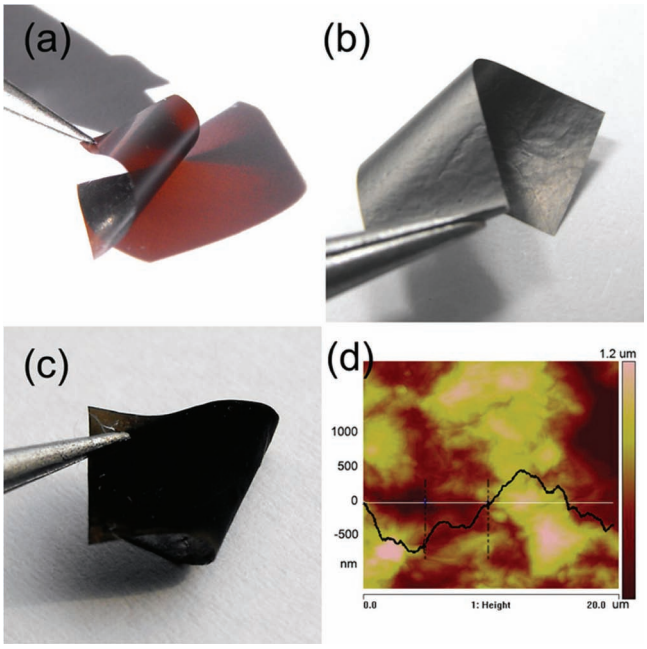

Figure 1. Optical images of a) a reddish-brown and sub-transparent GOP, b) a silver grey GP, and c) a black VACNT/GP film. d) An atomic force microscopy image of the GP surface.

and flexible. The GOP can be converted to GP by heat treatment. Figure 1b shows a reduced GP strip; we can see that the strip turns to silver gray in color and loses its original transparency. Four-point probe resistivity measurements showed a dramatic decrease of resistivity from ~1 MΩ/η for the GOP to ~50 Ω/η for the GP. The GP was then used as a substrate for growing VACNTs via CVD at 750 °C using ethylene as the carbon source and Fe nanoparticles as the catalyst. Figure 1c shows a hybrid film with VACNTs grown on the GP strip. It can be seen that the color of the strip turns to black, and the VACNT/GP film still demonstrates good flexibility. Even after being flexed 10 000 times, the VACNTs are still well anchored to the GP (See Figures S1 and S2, Supporting Information), indicating a strong adhesion between the grown VACNTs and the GP. We attribute this superb flexibility and durability to the highly flexible GP as shown in Figure 1b, the loose structure of the VACNTs, and desirable bonding between the VACNTs and the GP. We also conducted electrical measurement of the VACNT/GP film during the bending test. After 10 000 bending cycles, its resistivity increases by only 3.3%, showing excellent long-term stability (See Figure S1, Supporting Information).

Figure 2 shows scanning electron microscopy (SEM) images of the as-prepared VACNT/GP film. We can see from Figure 2a that the upper surface of the VACNTs is not flat, and the wavy morphology is a replication of the rough GP surface as shown in Figure 1d. Figure 2b shows the cross-section of the VACNT/GP film, and it can be seen that well-aligned CNTs with a height of tens of micrometers stand tidily on the GP. Figure 2c is an enlarged view of the VACNT/GP film cross-section demonstrating that the GP comprises layer-by-layer stacked graphene sheets. The curvature of the GP indicates that the stress generated during the VACNT growth can be released by deformation of the GP. We also found that the growth efficiency of VACNTs on the GP is higher than that on SiO_2/Si substrate as indicated by faster growth rate and prolonged catalyst lifetime (See Figure S3, Supporting Information), which can be attributed to the different surface morphology and physical properties of the substrates. To reveal the interface structure between the VACNTs and the GP, the VACNTs were partially peeled from the GP before SEM observation. Figure 2d shows that the remaining VACNTs are still intimately bonded to the GP without the influence of strong Van der Waals interactions from the neighboring CNTs during the peeling process, showing a strong bonding between the VACNTs and the GP. In Figure 2d, we can see that the VACNTs are not straight but curved. This is because a silicon wafer was put onto the GP to construct a "capped" configuration (See Figure S4, Supporting Information) during the CVD process, and thus a stress was applied to the growing CNTs.[19] The special curved structure may benefit the application of the VACNT/GP film in energy storage and conversion by providing added active sites. Transmission electron microscopy (TEM) observation (See Figure S5a, Supporting Information) shows a CNT ended with a Fe nanoparticles loaded on a graphene sheet, indicating that the VACNTs grow following a base-growth mode and the VACNTs connect well with the GP. Laser Raman spectra of the VACNTs and the GP (See Figure S5b, Supporting Information) display high I_D/I_G ratios, indicative of a high content of

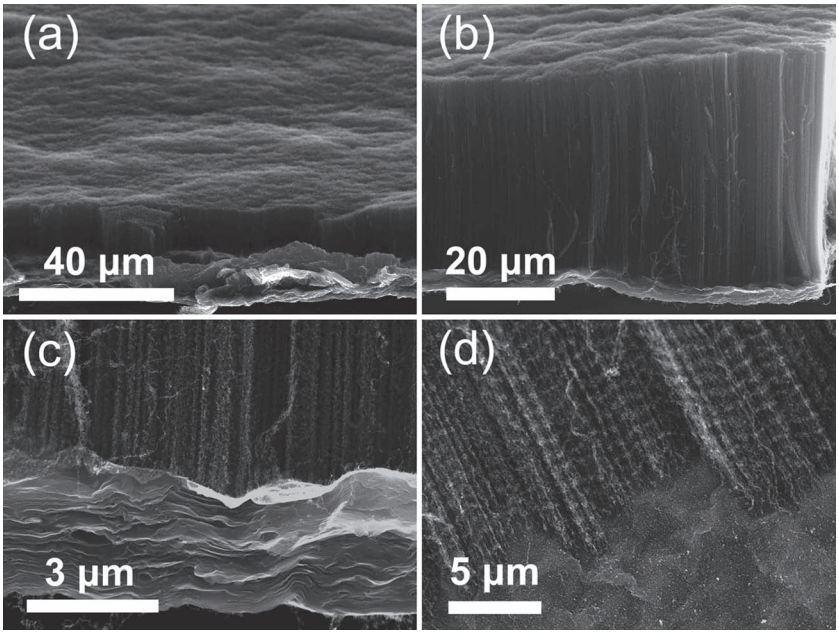

Figure 2. SEM images of the as-grown VACNTs on the GP. a) Top view of the VACNTs on the GP. b,c) Cross-section observation of the VACNT/GP film. d) Tilted-view showing the bonding between the VACNTs and the GP.

defects, which can be attributed to the low growth temperature of the VACNTs and the incomplete reduction of the GP.

LIBs are receiving increasing research interest due to their potential applications in portable electronics and hybrid electric vehicles. It is important to develop electrode materials with high-power performance for these applications.[20] CNTs, with their advantages of good electrical and thermal conductivity, high mechanical strength, and good flexibility, are good candidates as LIB electrode materials. Therefore, studies have been performed using CNTs as the electrode materials or as conducting additives in LIBs.[21] However, the cycling performance and high-rate capability of CNTs are not as satisfactory as expected,[22] possibly due to the large contact resistance of randomly packed CNTs. Since the VACNT/GP film reported here shows good flexibility and robustness, we utilized it directly as both the active anode material and the current collector of a LIB without adding any conducting binders.

Figure 3 shows the discharge capacity versus the cycle number for a cell with the VACNT/GP film as the anode. A stable discharge capacity of 290 mAh g^{-1} at 30 mA g^{-1} was achieved after 40 cycles, with a Coulombic efficiency of ~95%, which is higher than the values previously reported for random CNT films[23] or VACNTs on conducting PEDOT/PVDF films.[24] The bare GP exhibited a much lower reversible capacity of 155 mAh g^{-1} after 20 cycles (See Figure S6, Supporting Information). The rate performance of the VACNT/GP film was further investigated. When the current rate was increased step by step from 30 mA g^{-1} to 3.6 A g^{-1}, capacities of 265 and 55 mAh g^{-1} were achieved at 60 mA g^{-1} and 3.6 A g^{-1}, respectively. When the current rate was restored to 30 mA g^{-1}, even a slight increase (6.9%) in lithium storage capacity to 310 mAh g^{-1} was observed, indicating a good rate performance and excellent electrochemical stability of the VACNT/GP electrode. The high-rate capability can be attributed to the unique structure of the VACNT/GP electrode, where large numbers of transport paths are provided by the VACNTs rooted firmly on the conducting GP. Although the capacity of the VACNT/GP electrode is somehow lower than some types of novel carbons, the most highlighted advantage of such a hybrid carbon electrode for LIB is the integration of conductive active materials with flexible and stable current collector. Since the VACNT/GP electrode is free from any foreign additives and the GP current collector is much more lighter than the commonly used copper foil, the whole weight of the anode can be largely reduced, which leads to an increased capacity per battery unit. Moreover, the superb chemical/electrochemical stability of the copper-free VACNT/GP electrode may also contribute to the long-term stability and safety of LIBs, which are critical for application in vehicles.[25] The easy handling of the copper-free VACNT/GP electrode also presents a solution for flexible energy storage devices. It is worth noting that the capacity of the VACNT/GP electrode can be further improved by introducing additional substances, such as silicon, by filling in the hollow core or decorating the surface of the VACNTs, so that a combined high-rate and high-capacity performance can be achieved simultaneously.

DSSCs show promise as next-generation solar cells arising from their high light-to-electricity conversion efficiency and low fabrication cost and potential to be integrated into flexible devices. Typically, a DSSC comprises a dye-sensitized nanocrystalline titanium dioxide electrode, electrolyte solution usually with a dissolved iodide/triiodide (I^-/I_3^-) redox couple between the electrodes, and a counter electrode (See Figure S7, Supporting Information). The counter electrode of the DSSC, whose function is to transfer electrons arriving from the external circuit back to the redox electrolyte and to catalyze the reduction of the I_3^-, is usually made of platinum (Pt). However, Pt is a scarce resource and is very expensive. Thus, CNTs have been considered as a potential candidate for replacing traditional Pt counter electrodes in DSSCs,[26–29] given their large surface area, high electrical conductivity and good catalytic activity.

In this study, we used the VACNT/GP film directly as the counter electrode of the DSSCs, and we compared in parallel the performances obtained for the pure GP, tangled CNTs (TCNT)/GP film, VACNT/GP film and Pt counter electrodes. **Figure 4** illustrates the photocurrent-voltage curves of these four kinds of DSSCs. The open-circuit voltage (V_{oc}), short-circuit photocurrent density (J_{sc}), fill factor (FF) and energy conversion efficiency (η) of the cells are listed in Table S1 (Supporting Information). It can be seen that the DSSC using the bare GP electrode performed poorly, the photovoltaic parameters being J_{sc} of 13.87 mA cm^{-2}, V_{oc} of 600 mV, FF of 0.181 and conversion efficiency (η) of 1.50%. The low FF is consistent with the poor

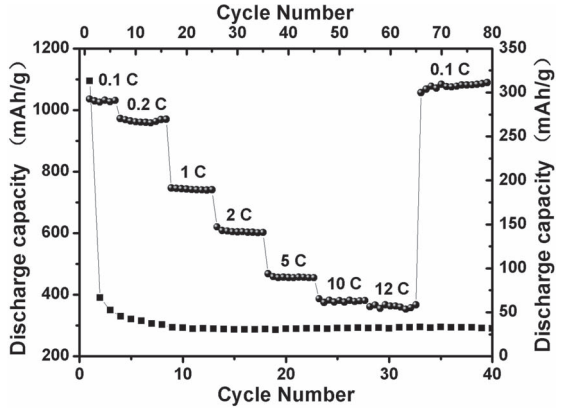

Figure 3. Cyclic performance and high-rate capability of the VACNT/GP film anode of a LIB.

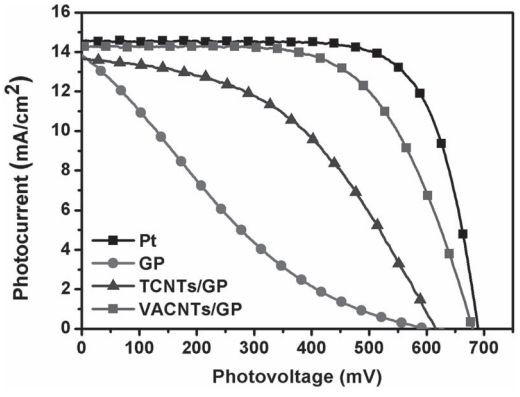

Figure 4. Current-voltage characteristics of four DSSCs using the Pt, GP, TCNT/GP film, and VACNT/GP film as counter electrodes.

catalytic activity of the GP to the reduction of I_3^- and large charge transfer resistance (R_{ct}) at the electrolyte/electrode interface (See Table S2, Supporting Information). The necessity of depositing an effective catalyst onto the GP can easily be appreciated. As shown in Figure 4 and Table S1 (Supporting Information), the catalytic properties are improved by coating a CNT layer onto the flexible GP. It can be seen that DSSCs with the TCNT/GP film and the VACNT/GP film exhibit higher η of 3.88% and 6.05%, respectively. Compared with the performance of the DSSC with bare GP counter electrode, the most pronounced change of DSSCs with the CNT/GP film counter electrodes is the FF, while the corresponding values (J_{sc}, V_{oc}, FF and η) of the Pt counter electrode are 14.59 mA cm^{-2}, 689 mV, 0.725 and 7.29%, respectively.

The efficiency of the DSSC using the VACNT/GP film as counter electrode reached 83% of that with a Pt film electrode. The decrease of FF of the DSSCs with the GP-based electrodes is due to the higher series resistance of the GP and higher charge transfer resistance as listed in Table S2 (Supporting Information). The resistivity of the GP is 50 Ω/□, much larger than 0.5 Ω/□ for the Pt electrode. The electrochemical impedance spectra (EIS) results also show the DSSCs with the GP based counter electrodes have higher resistances (See Figure S9, Supporting Information). When compared to the TCNT/GP film and the GP, the VACNT/GP film shows superior FF, J_{sc} and V_{oc} for the cells. This is mainly because that the VACNTs, which are perpendicularly rooted onto the GP, can provide shortest transportation paths for the electrons. Park et al. studied the permeability of porous media by modeling, and pointed out that the effective permeability is doubled for the fiber orientation parallel with the mean flow direction, when compared to the case of the fibers normal to the mean flow direction.[30] Therefore, the well-aligned CNTs can also facilitate the ion (I_3^-) transportation efficiently and decrease the charge transfer resistance. As shown in Table S2 (Supporting Information), the charge transfer resistance at the interface between electrolyte and the VACNT/GP film is smaller than that at the TCNT/GP film and the GP interfaces. In combination with its good flexibility, the hybrid VACNT/GP film shows potential for use in DSSCs for portable electronics by replacing the Pt counter electrode.

In summary, VACNTs were directly grown on the GP by a thermal CVD method. The as-prepared freestanding VACNT/GP film was employed as an integrated electrode combining both active component and current collector for LIB, and good high-rate capability and cycling performance were demonstrated. When served as the counter electrode of a DSSC, the VACNT/GP film displayed superior overall performance to the GP and the TCNT/GP films and slightly lower efficiency when compared with the Pt electrode. Due to its good electrical conductivity, high thermal and chemical stability, and desirable flexibility, the VACNT/GP film may find applications in high-performance, flexible energy storage and conversion devices.

Experimental Section

Thermal annealing of GOP: The rectangular GOP strips were sandwiched between two silicon pads and placed in the center of a quartz tube inside a horizontal tubular furnace. Then the furnace was heated to 200 °C at a rate of 2 °C min^{-1} in an atmosphere of 1 Torr of H_2.

CVD growth of VACNTs: 5 nm Al_2O_3 and 1 nm Fe were sequentially deposited on the GP as catalyst by using an ion-beam coating apparatus (Gatan PECS 681). A silicon wafer was put onto the upper surface of the GP to tune the local gas flow conditions (See Figure S4, Supporting Information). CNT growth was conducted in a horizontal quartz tube with an inner diameter of 1 inch. The VACNTs were prepared by using C_2H_4 as carbon source and H_2 and Ar as carrier gases with an $Ar/H_2/C_2H_4$ flux of 200/120/60 sccm. The synthesis temperature was 750 °C. After the growth process, the product was cooled naturally to room temperature under a protective Ar/H_2 atmosphere.

LIB assembly and testing: A hybrid film comprising ~500 μm thick VACNTs grown on a ~3 μm thick GP was used as the anode of a LIB for testing. The weight ratio of VACNTs in the VACNT/GP hybrid material is ~65%. The electrochemical measurements were carried out using button-type two-electrode half cells at room temperature. The cells were assembled in an Ar-filled glove box (MBraun, Unilab) with the concentration of vapor and oxygen below 1 ppm. Lithium metal was used as counter electrode, Celgard 2400 as separator and 1 M $LiPF_6$ dissolved in a 1:1:1 (v/v/v) mixture of ethylene carbonate, propylene carbonate and dimethyl carbonate as electrolyte solution. The cells were galvanostatically charged and discharged at a fixed voltage window between 0.001 V and 2.5 V versus Li^+/Li. The cycling performance of the VACNT/GP film was studied at a current rate of 0.1 C (1C = 300 mA g^{-1}). The cyclic voltammogram of the VACNT/GP film was tested in the voltage range of 0.001–3.0 V (vs. Li^+/Li) at a scan rate of 0.1 mV s^{-1}.

DSSC device fabrication and photovoltaic measurements: For DSSC assembly and testing, a hybrid film containing ~100 μm thick VACNTs grown on a ~3 μm thick GP was used as the counter electrode. Nanocrystalline TiO_2 films were deposited on fluorine-doped SnO_2 conducting glass substrates (15 Ω/□) by screen-printing a TiO_2 (Degussa P25) paste. The thickness of the films were controlled to be about 15 μm by repeating screen-printing the paste. The TiO_2 films were heated to 450 °C and sintered for 30 min, then cooled to ~80 °C and immersed into ethanol solution of N719 ($[RuL_2(NCS)_2]$:2TBA, L = 2,2'-bipyridyl-4,4'-dicarboxylic acid, TBA = tetra-*n*-butylammonium) dye at room temperature for at least 12 h. The electrolyte consisted of 0.6 M methylhexylimidazolium iodide, 0.05 M iodine, 0.1 M LiI and 0.5 M tert-butylpyridine in 3-methoxypropionitrile. An open sandwich-type cell, which was not sealed, was fabricated in air by clamping the sensitized TiO_2, a drop of electrolyte and a counter electrode with two clips. The active electrode area was 0.15 cm^2. The photocurrent-voltage measurements were recorded by a potentiostat (Princeton Applied Research, Model 263A). A solar light simulator (Oriel, 91192) was used as the white light source to give AM 1.5 illumination on the surface of the solar cells. The intensity of incident light was measured with a radiant power/energy meter (Oriel, 70260) before each experiment.

Supporting Information

Supporting Information is available from the Wiley Online Library or from the author.

Acknowledgements

We acknowledge financial support from Ministry of Science and Technology of China (Grants 2011CB932601, 2011CB932604, 2009AA03Z337, and 2008DFA51400), and National Natural Science Foundation of China (Grants 90606008, 50872137, 50921004, 20725311, and 50972101).

Received: January 1, 2011
Revised: March 11, 2011
Published online: April 26, 2011

[1] K. Kordas, G. Toth, P. Moilanen, M. Kumpumaki, J. Vahakangas, A. Uusimaki, R. Vajtai, P. M. Ajayan, *Appl. Phys. Lett.* **2007**, *90*, 123105.
[2] V. L. Pushparaj, M. M. Shaijumon, A. Kumar, S. Murugesan, L. Ci, R. Vajtai, R. J. Linhardt, O. Nalamasu, P. M. Ajayan, *Proc. Natl. Acad. Sci. USA.* **2007**, *104*, 13574.
[3] D. N. Futaba, K. Hata, T. Yamada, T. Hiraoka, Y. Hayamizu, Y. Kakudate, O. Tanaike, H. Hatori, M. Yumura, S. Iijima, *Nat. Mater.* **2006**, *5*, 987.
[4] L. Qu, L. Dai, *Adv. Mater.* **2007**, *19*, 3844.
[5] X. B. Zhang, K. L. Jiang, C. Teng, P. Liu, L. Zhang, J. Kong, T. H. Zhang, Q. Q. Li, S. S. Fan, *Adv. Mater.* **2006**, *18*, 1505.
[6] S. Talapatra, S. Kar, S. K. Pal, R. Vajtai, L. Ci, P. Victor, M. M. Shaijumon, S. Kaur, O. Nalamasu, P. M. Ajayan, *Nat. Nanotechnol.* **2006**, *1*, 112.
[7] L. B. Zhu, Y. Y. Sun, D. W. Hess, C. P. Wong, *Nano Lett.* **2006**, *6*, 243.
[8] M. J. Kim, N. Nicholas, C. Kittrell, E. Haroz, H. W. Shan, T. J. Wainerdi, S. Lee, H. K. Schmidt, R. E. Smalley, R. H. Hauge, *J. Am. Chem. Soc.* **2006**, *128*, 9312.
[9] T. Hiraoka, T. Yamada, K. Hata, D. N. Futaba, H. Kurachi, S. Uemura, M. Yumura, S. Iijima, *J. Am. Chem. Soc.* **2006**, *128*, 13338.
[10] A. K. Geim, K. S. Novoselov, *Nat. Mater.* **2007**, *6*, 183.
[11] A. K. Geim, *Science* **2009**, *324*, 1530.
[12] D. H. Lee, J. E. Kim, T. H. Han, J. W. Hwang, S. Jeon, S. Y. Choi, S. H. Hong, W. J. Lee, R. S. Ruoff, S. O. Kim, *Adv. Mater.* **2010**, *22*, 1247.
[13] D. H. Lee, J. A. Lee, W. J. Lee, S. O. Kim, *Small* **2011**, *7*, 95.
[14] H. Y. Jeong, D. S. Lee, H. K. Choi, D. H. Lee, J. E. Kim, J. Y. Lee, W. J. Lee, S. O. Kim, S. Y. Choi, *Appl. Phys. Lett.* **2010**, *96*, 213105.
[15] R. K. Paul, M. Ghazinejad, M. Penchev, J. A. Lin, M. Ozkan, C. S. Ozkan, *Small* **2010**, *6*, 2309.
[16] L. L. Zhang, Z. G. Xiong, X. S. Zhao, *ACS Nano* **2010**, *4*, 7030.
[17] Z. J. Fan, J. Yan, L. J. Zhi, Q. Zhang, T. Wei, J. Feng, M. L. Zhang, W. Z. Qian, F. Wei, *Adv. Mater.* **2010**, *22*, 3723.
[18] C. M. Chen, Q. H. Yang, Y. G. Yang, W. Lv, Y. F. Wen, P. X. Hou, M. Z. Wang, H. M. Cheng, *Adv. Mater.* **2009**, *21*, 3007.
[19] A. J. Hart, A. H. Slocum, *Nano Lett.* **2006**, *6*, 1254.
[20] C. Liu, F. Li, L. P. Ma, H. M. Cheng, *Adv. Mater.* **2010**, *22*, E28.
[21] B. J. Landi, M. J. Ganter, C. D. Cress, R. A. DiLeo, R. P. Raffaelle, *Energy Environ. Sci.* **2009**, *2*, 638.
[22] H. Zhang, G. P. Cao, Y. S. Yang, *Energy Environ. Sci.* **2009**, *2*, 932.
[23] G. Maurin, F. Henn, B. Simon, J. F. Colomer, J. B. Nagy, *Nano Lett.* **2001**, *1*, 75.
[24] J. Chen, Y. Liu, A. I. Minett, C. Lynam, J. Z. Wang, G. G. Wallace, *Chem. Mater.* **2007**, *19*, 3595.
[25] S. Hossain, Y. Saleh, R. Loutfy, *J. Power Sources* **2001**, *96*, 5.
[26] Y. H. Luo, D. M. Li, Q. B. Meng, *Adv. Mater.* **2009**, *21*, 4647.
[27] E. Ramasamy, W. J. Lee, D. Y. Lee, J. S. Song, *Electrochem. Commun.* **2008**, *10*, 1087.
[28] K. Suzuki, M. Yamaguchi, M. Kumagai, S. Yanagida, *Chem. Lett.* **2003**, *32*, 28.
[29] J. E. Trancik, S. C. Barton, J. Hone, *Nano Lett.* **2008**, *8*, 982.
[30] J. Park, M. Matsubara, X. Li, *J. Power Sources* **2007**, *173*, 404.